Spike-count distribution in a neuronal population under weak common stimulation

Alexandra Kruscha and Benjamin Lindner
Bernstein Center for Computational Neuroscience Berlin and Institute of Physics, Humboldt University Berlin, Germany
(Received 27 July 2015; published 30 November 2015)

We study the probability distribution of the number of synchronous action potentials (spike count) in a model network consisting of a homogeneous neural population that is driven by a common time-dependent stimulus. We derive two analytical approximations for the count statistics, which are based on linear response theory and hold true for weak input correlations. Comparison to numerical simulations of populations of integrate-and-fire neurons in different parameter regimes reveals that our theory correctly predicts how much a weak common stimulus increases the probability of common firing and of common silence in the neural population.

DOI: 10.1103/PhysRevE.92.052817 PACS number(s): 89.75.Fb, 87.10.Ca, 87.18.Tt

I. INTRODUCTION

Effects of noise in nonlinear dynamical systems are relevant in various scientific disciplines [1–3]. They are often surprising and challenging to analyze. Of special interest in many systems is the influence of global fluctuations, so-called common noise, that act on a whole group or network of nonlinear elements. Common noise can arise in different situations, e.g., from global weather conditions for populations dynamics in the case of the celebrated Moran effect [4], by temperature fluctuations [5] or by coupling [6] in the case of chemical reactions in spatially separated compartments such as cells, or by spatially extended sensory signals in neural systems [7].

Theoretical studies have revealed that even in the simple case of uncoupled elements, common noise can lead to nontrivial effects such as strong synchronization of nonlinear oscillators [8–12] or temporal oscillations [13,14]. If statistically identical elements are subject to a common noisy stimulus, such a scenario can be also interpreted differently: the time series of the elements can be regarded as a collection of response trials to one and the same frozen input signal. In this spirit, common noise has been used to test the response consistency of nonlinear systems such as lasers [15] or nerve cells [16].

We illustrate this simple setup in Fig. 1 for the case of a neural population, i.e., a group of uncoupled elements, each of which obeys highly nonlinear (spike-generating) dynamics. All neurons are subject to a common stimulus and in addition to individual independent noise. To calculate statistical measures for this common-noise problem has particular importance for at least three reasons.

First, the aforementioned response consistency is of special interest in the neural context because one major role of sensory neurons is to encode information about time-dependent signals. Hence, it is of great interest how reliable they can respond to repeated presentations of the same stimulus in the face of complex neural dynamics and intrinsic noise sources [16–18]. Second, common noise is shaping the spontaneous activity of the neural networks of the brain: nerve cells are subject to common stimuli due to shared input and cross-correlations between neurons [19]. How these sources affect correlations in recurrent networks is still debated [20]. Third, in the neural periphery common stimuli emerge from complex time-dependent sensory signal, which influences many (often uncoupled) cells in the same way [21]. In this case, it has been explored how strongly such a common noise will be encoded in the synchronous activity of the population [22,23].

The statistics of the activity of a neural population receiving a common external signal has been in the focus of several studies. Expressions of the activity distribution have been derived by Amari *et al.* [24] for simple dichotomized Gaussian (DG) neurons in the limit of infinite large populations. Recently, Leen *et al.* [25] showed that when matching the mean firing rate and correlation between two neurons, the DG-model gives a good estimation of the activity distribution of populations of the more complicated exponential integrate-and-fire (EIF) neuron model. These results still require computational fitting of model parameters.

In this paper, we derive explicit results for the activity distribution for the case of weak common noise, an assumption that seems to be reasonable at least in some situations [26]. Our results may contribute to a more general theory of how sensory information is encoded in the synchronous activity of neural populations.

II. MODEL AND STATISTICS OF INTEREST

We aim at an explicit analytical expression of the spike count distribution of a neural population, which is driven by a common stimulus. Specifically, we consider a homogeneous population of N leaky integrate-and-fire neurons, each of which obeys the voltage dynamics ($k \in \{1,\dots,N\}$),

$$\dot{v}_k = -v_k + \mu + \sqrt{2D}\{\sqrt{1-c}\,\xi_k(t) + \sqrt{c}\,\xi_0(t)\}, \quad (1)$$

where μ is the constant base current, ξ_j, $j \in \{0,\dots,N\}$, are independent white noise processes with correlation function $\langle \xi_j(t)\xi_{j'}(t')\rangle = \delta_{j,j'}\delta(t-t')$, D is the total noise intensity, and $c \in [0,1]$ is the correlation coefficient of the input current (see Fig. 1 for a sketch of the model). Whenever the voltage v_k exceeds the threshold one, a spike is recorded and v_k is reset to zero. The corresponding spike trains are $x_k(t) = \sum_i \delta(t - t_{k,i})$, where the $t_{k,i}$ are the spike times of the kth neuron. The average firing rate r_0 of each neuron is the mean value of the spike train $r_0 = \langle x_k \rangle_{\xi_k,\xi_0}$.

By $s(t) = \sqrt{2Dc}\,\xi_0(t)$ we denote the common stimulus each neuron is receiving. The input correlation coefficient c determines the fraction of the total noise each neuron receives, which is common to the entire population. It determines how large the common external stimulus is in comparison to the

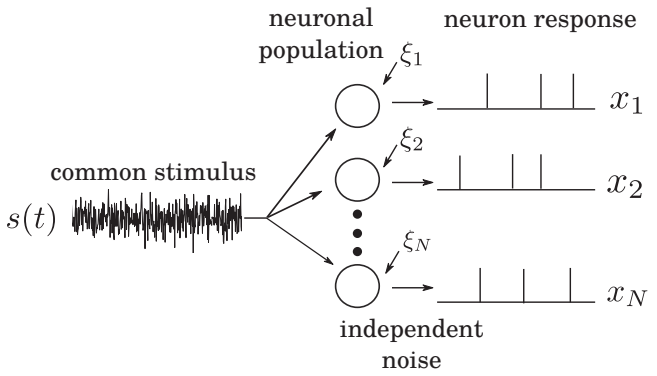

FIG. 1. Schematic representation of the model. A homogeneous population of N neurons is subject to a common stimulus and independent noise, leading to variable single neuron output spike trains $x_k(t)$.

independent intrinsic fluctuations. For $c = 0$, i.e., when there is no common stimulus, all neurons are completely independent. For $c = 1$, the independent fluctuations vanish such that every neuron in the population receives exactly the same input and thus behaves asymptotically (in the long-time limit) exactly the same way.

The *population activity* A within a time interval $I_\Delta := [t - \Delta, t]$ of width Δ refers to the fraction of active neurons, i.e., the total number of spikes of the population within this interval divided by the population size [27]. Formally, the spike counts can be expressed by integrals over the spike trains:

$$A = \frac{1}{N}\sum_{k=1}^{N}\int_{t-\Delta}^{t} x_k(t')dt'. \tag{2}$$

If Δ is sufficiently small, the population activity can be regarded as a proxy of synchronous behavior, as can be seen in Fig. 2. If $A(t) = 0$, then there is no spike within I_Δ, whereas $A(t) = 1$ corresponds to the case where all neurons fire "simultaneously" within this time bin. Of course, even in the absence of coupling and correlated input, neurons fire together by chance and it is an interesting question how this baseline "synchronization" is influenced by common

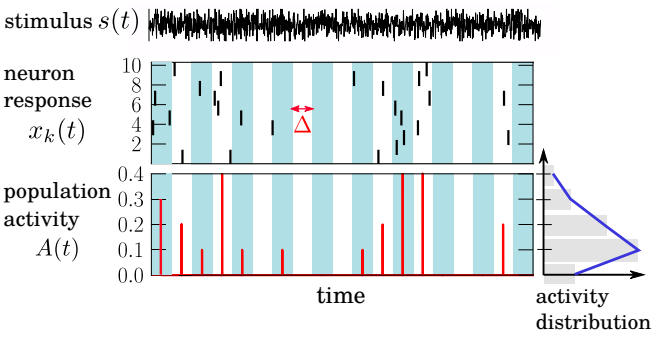

FIG. 2. (Color online) Population activity. Spike trains of $N = 10$ LIF neurons receiving independent noise and a common stimulus $s(t)$ (low-pass filtered for illustration). The population activity is the fraction of active neurons of a population within a time bin of width Δ.

noise. Here, we are not interested in the time-dependent features of the population activity, but solely in its statistical distribution p_A.

Before we start with any analytical consideration, we show in Fig. 3(a) simulation results for the distribution p_A for a moderately sized population ($N = 30$) and different values of the input correlation c. With increasing correlation, the density changes from a narrow unimodal to a bimodal distribution (previously discussed for a similar setup in Ref. [24]). The shift of probability toward the extremes can be regarded as the synchronizing effect of the common noise, resulting in common firing ($A = 1$) and common silence ($A = 0$).

To extract the synchrony that is solely induced by the common noise, it is revealing to subtract from the activity distribution the independent baseline activity [see Fig. 3(b)]. For our analytical calculations, we focus on the weak correlation regime ($c \ll 1$), in which linear response theory can be applied to approximate the distribution p_A.

III. GENERAL THEORETICAL CONSIDERATIONS

In the following, we consider the width of the interval, Δ, to be substantially smaller than the mean interspike interval, $1/r_0$, i.e., the probability for one neuron to spike more than once in I_Δ is negligible. Hence, the individual neuron either spikes with probability R or it does not spike with probability $1 - R$. For a fixed realization s of the common stimulus every neuron in the population spikes within I_Δ with some probability $R[s]$ and all neurons are statistically independent of each other. Here, $R[s] = R[s(t'), t' \leqslant t]$ is a functional of a single realization s up to time t due to causality. Because the spiking probability $R[s]$ is the same for each neuron, the number of active neurons in I_Δ obeys a binomial distribution $\mathrm{Bin}(N, R[s])$. To obtain the distribution of the population activity A, this conditional probability has to be averaged over all possible realizations of the stimulus:

$$\mathbb{P}\left(A = \frac{m}{N}\right) = \left\langle \binom{N}{m} (R[s])^m (1 - R[s])^{(N-m)} \right\rangle_s. \tag{3}$$

This equation has already been used for special neuron models in Refs. [24,25]. The probability in Eq. (3) corresponds to the total probability for each possible activity $A = m/N$, where $m \in \{0, 1, \ldots, N\}$. In order to get a probability density p_A for A, such that

$\mathbb{P}(A) = p_A(A)\Delta A$ with $\Delta A = 1/N$, Eq. (3) must be multiplied by $1/\Delta A = N$:

$$p_A(A) = N\binom{N}{AN}\langle [(R[s])^A (1 - R[s])^{(1-A)}]^N \rangle_s. \tag{4}$$

How to perform the average over all stimulus realizations is a nontrivial problem because one must specify $R[s]$. We approximate $R[s]$ for a weak stimulus in Sec. IV. Alternatively, one can incorporate the stochasticity of s into R directly: R can be interpreted as a random variable with probability density p_R. If this density is known, we can express the probability density Eq. (4) by

$$p_A(A) = N\binom{N}{AN}\int_0^1 [R^A (1 - R)^{(1-A)}]^N p_R(R) dR. \tag{5}$$

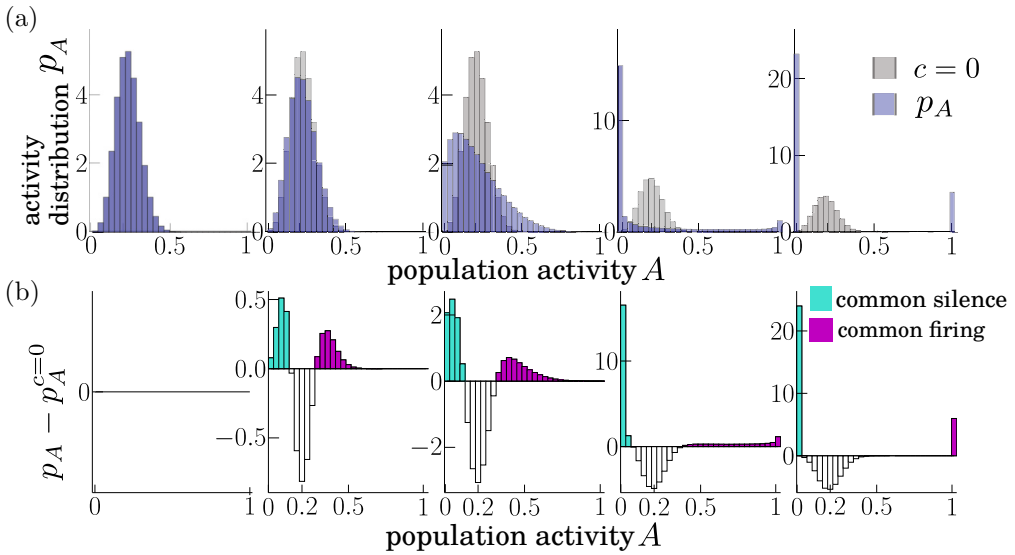

FIG. 3. (Color online) Synchronizing effect of common noise. (a) Activity distribution for different values of the input correlation c (from left to right: $c = 0.0, 0.05, 0.4, 0.99, 1.0$). (b) Respective difference of the activity distribution to the stimulus-free distribution ($c = 0$). Parameters: $N = 30, \mu = 1.2$, $D = 0.2$, $\Delta = 0.25$.

This means, that one only needs to know the distribution of the single neuron spiking probability within a time bin, I_Δ, conditioned on the common stimulus. Then, using Eq. (5), one can analytically compute the distribution of the population activity.

It is instructive to consider the limiting cases for the distribution of the stimulus-conditioned firing rate, p_R. In the absence of correlation ($c = 0$), the firing rate is not modulated by a common stimulus, such that $p_R = \delta(R - R_0)$, where $R_0 = r_0\Delta$ is the mean firing probability within I_Δ. For full correlation ($c = 1$), i.e., in the absence of independent noise, the probability to spike is either one or zero, such that $p_R(R) = (1 - R_0)\delta(R) + R_0\delta(R - 1)$. The transition between these extremes of p_R for different input correlation is sketched in Fig. 4(a) with the corresponding activity distributions in Fig. 4(b).

An important connection between p_R and p_A is

$$p_R = \lim_{N\to\infty} p_A. \tag{6}$$

This relation is obtained from Eq. (5), using that the binomial distribution converges to a normal distribution, which in turn approaches a δ function in the limit of infinite N:

$$\lim_{N\to\infty} N\binom{N}{AN}(R^A(1-R)^{(1-A)})^N = \delta(A - R). \tag{7}$$

An intuitive way of deriving Eq. (6) is to think about how we can measure p_R. If we fix a stimulus realization and simulate the response of a single neuron in n trials, we can perform an average over the intrinsic noise. For a chosen time bin, I_Δ, we then obtain the firing probability $R[s]$ by adding up the spikes

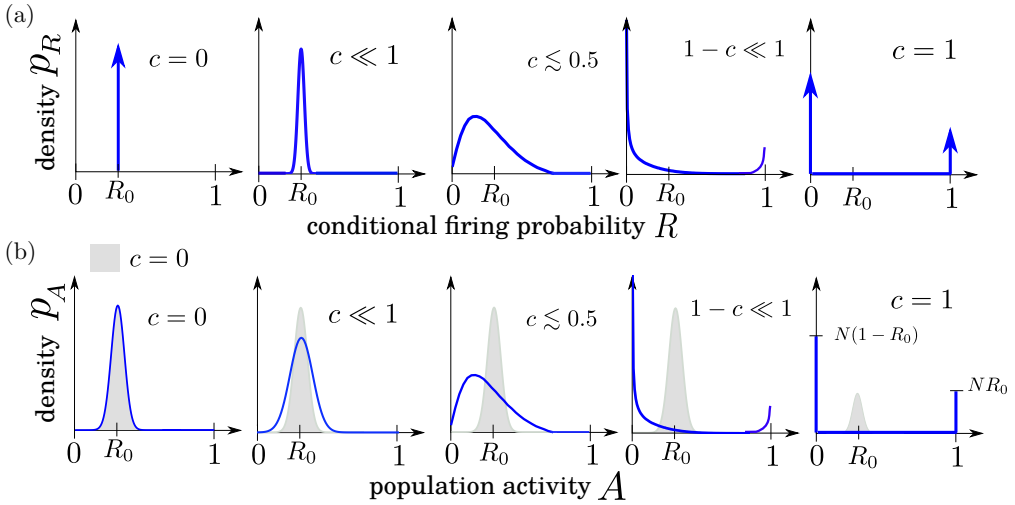

FIG. 4. (Color online) Sketch of the qualitative change in the distributions of p_R and p_A for varying input correlation c. Probability density of the stimulus-conditioned and windowed firing rate (a) and the corresponding population activity distributions (b). For comparison p_A of the stimulus free case ($c = 0$) is shown in shaded gray. The latter sketch should be compared to the simulation results shown in Fig. 3(b).

of all n trials within this interval and divide it by n. This value is indeed nothing but the activity within I_Δ of a population of size $N = n$ driven by s. Hence, in order to numerically estimate the distribution of R, one simply measures the distribution (average over many realizations s) of the activity A for a very large value of N.

In the following two sections we present approximations for p_R and p_A for the case of a weak common stimulus.

IV. APPROXIMATING THE DISTRIBUTION OF THE CONDITIONAL FIRING PROBABILITY

The probability that a single neuron spikes within $[t-\Delta, t]$, given a fixed realization of the common stimulus $s(t')$ with $t' \leqslant t$ is given by

$$R[s] = \int_{t-\Delta}^{t} r(t')dt', \tag{8}$$

where $r(t) = \langle x_k(t)\rangle_{\xi_k}$ is the instantaneous firing rate of a single neuron for a fixed stimulus s. In other words, R is the windowed firing rate, which is time-dependent due to the common stimulus. For a weak stimulus, the instantaneous firing can be approximated by the linear response relation

$$r(t) = r_0 + K * s(t), \tag{9}$$

where $K(t)$ is the linear response function and the average firing rate for an LIF is given by [28]

$$r_0 = \left[\sqrt{\pi}\int_{(\mu-1)/\sqrt{2D}}^{\mu/\sqrt{2D}} e^{y^2}\operatorname{erfc}(y)dy\right]^{-1}. \tag{10}$$

The asterisk in Eq. (9) stands for the convolution $K * s = \int_{-\infty}^{\infty} s(t')K(t-t')dt'$. Using Eq. (8) and Eq. (9) yields

$$R[s] = r_0\Delta + \int_{t-\Delta}^{t} K * s(t')dt' = R_0 + \sqrt{c}\,\hat{s}(t). \tag{11}$$

We recall that $R_0 = r_0\Delta$ denotes the firing probability of a stimulus-free neuron ($c = 0$) within I_Δ. The effective stimulus, $\sqrt{c}\,\hat{s} = \int_{t-\Delta}^{t} K * s(t')dt'$, modulates the firing probability; in the definition of $\hat{s}$ we extracted the explicit dependence on the input correlation c. The integral operator $\int_{t-\Delta}^{t} \bullet dt'$ can be written alternatively by a convolution with the boxcar function $\mathcal{B}(t) = \theta(t+\Delta) - \theta(t)$,

$$\sqrt{c}\,\hat{s} = \mathcal{B} * K * s. \tag{12}$$

Because the convolution is a linear operation (for fixed t, the random variable $\hat{s}$ is a linear functional of the process s) and the stimulus is a Gaussian process, the stochastic process $\hat{s}$ is Gaussian as well. It is centered around zero, i.e., $\langle\hat{s}\rangle_s = 0$, and its variance is given by the integral over its power spectrum,

$$\begin{aligned}\langle\hat{s}^2\rangle_s &= \int_{-\infty}^{\infty} |\tilde{B}\tilde{K}|^2 \frac{S_{s,s}(f)}{c}df \\ &= 2D\Delta^2\int_{-\infty}^{\infty} \operatorname{sinc}^2(\Delta\pi f)|\chi(f)|^2 df,\end{aligned} \tag{13}$$

where a tilde stands for the Fourier transform and $\operatorname{sinc}(x) = \sin(x)/x$. The power of each frequency component of the common stimulus is given by $S_{s,s} = 2Dc$ and $\chi = \tilde{K}$ is the susceptibility of the firing rate of a neuron driven by $\mu + 2D\xi(t)$, which, for the LIF-neuron, can be expressed in terms of parabolic cylinder functions $\mathcal{D}_\alpha(z)$ [29]:

$$\chi(f) = \frac{r_0 2\pi i f}{\sqrt{D}(2\pi i f - 1)} \frac{\mathcal{D}_{2\pi i f-1}\left(\frac{\mu-1}{\sqrt{D}}\right) - e^{\Delta}\mathcal{D}_{2\pi i f-1}\left(\frac{\mu}{\sqrt{D}}\right)}{\mathcal{D}_{2\pi i f}\left(\frac{\mu-1}{\sqrt{D}}\right) - e^{\Delta}\mathcal{D}_{2\pi i f}\left(\frac{\mu}{\sqrt{D}}\right)} \tag{14}$$

(equivalent expressions in terms of hypergeometric functions can be found in Ref. [30]). The variance $\langle\hat{s}^2\rangle_s$ can be therefore computed analytically and does not include any fitting parameters. In conclusion, if one assumes a linear response of the instantaneous firing rate, the probability density distribution of R is given by

$$\hat{p}_R(R) = \frac{1}{\sqrt{2\pi c\langle\hat{s}^2\rangle_s}}\exp\left[\frac{-(R_0-R)^2}{2c\langle\hat{s}^2\rangle_s}\right] = \mathcal{N}(R_0, c\langle\hat{s}^2\rangle_s). \tag{15}$$

This normal distribution has to be regarded as a coarse approximation for p_R. It has one clear limitation: as a probability, R is supposed to take values only on $[0,1]$, whereas the density in Eq. (15) is formally distributed (and normalized) on $\mathbb{R}$. However, if $\hat{s}$ is small enough, the main support of $\hat{p}_R$ will be on $[0,1]$.

In Fig. 5 we compare the linear response approximation Eq. (15) with the numerically measured $p_R(R)$ for various

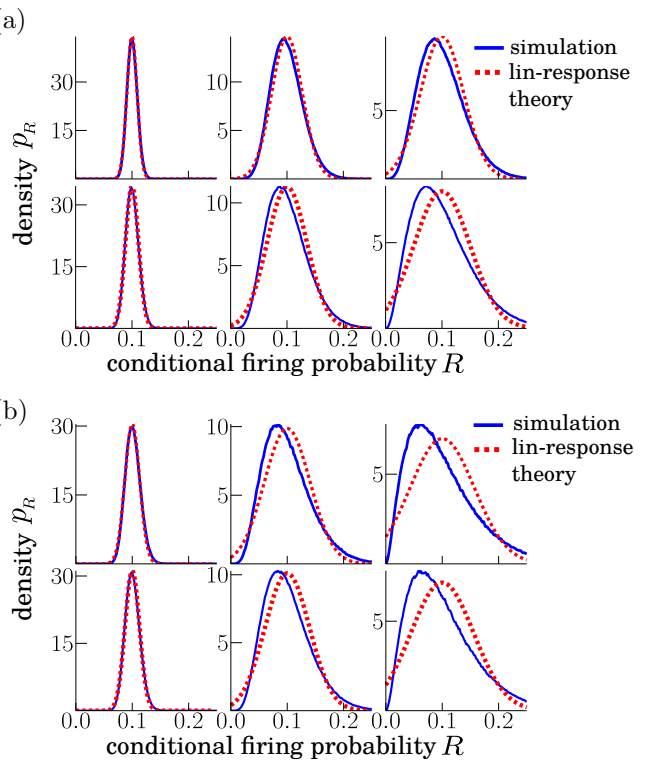

FIG. 5. (Color online) Probability distribution of the stimulus-conditioned firing rate. Simulation results are compared to the linear response approach Eq. (15) in the suprathreshold regime with $\mu = 1.2$ (a) and in the subthreshold regime with $\mu = 0.9$ (b) for different values of the input correlation c (from left column to right: $c = 0.001, 0.1, 0.2$) for total noise intensity $D = 0.01$ (top row) and $D = 0.1$ (bottom row), respectively. Remaining parameters: $R_0 = r_0\Delta = 0.1$.

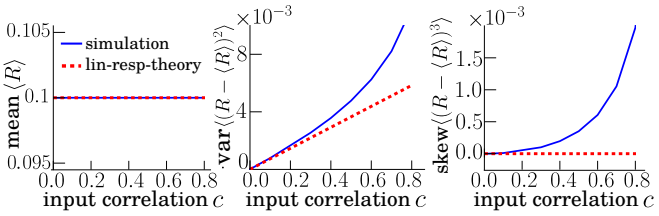

FIG. 6. (Color online) First three central moments of the stimulus-conditioned rate vs. input correlation. Simulation results (blue solid) compared to linear response approximation (red dashed). Parameters: $D = 0.01$, $\mu = 1.2$.

parameter settings. For all plots, $R_0 = 0.1$ and the bin width Δ is adjusted such that $r_0\Delta = R_0$. For weak common noise ($c = 0.01$), the normal distribution Eq. (15) provides an adequate description both in the suprathreshold regime, i.e., where the mean current μ is larger than the firing threshold, such that the system is in the tonic firing regime [Fig. 5(a)], as well as in the subthreshold regime, i.e., the mean current is below threshold, such that noise is necessary to induce firing [Fig. 5(b)]. For higher input correlations c, the distribution of R differs from a Gaussian. In particular, the density becomes significantly skewed. This is not surprising if we think of the bimodal shape that the density approaches for strong correlations, cf. our discussion of Fig. 4(a).

In Fig. 6 we compare the first three moments of the density p_R from numerical simulations to the linear response prediction $\hat{p}_R$. While the mean value remains R_0 [Fig. 6(a)], the variance first increases in a linear fashion with the input correlation c but shows a stronger growth for larger c [Fig. 6(b)]. The skewness of the density increases [Fig. 6(c)] in a nonlinear fashion.

V. APPROXIMATIONS OF THE ACTIVITY DISTRIBUTION

Combining the general result for the activity distribution with the linear response result from the previous section yields an integral expression for p_A. In the following we also derive a simpler Gaussian approximation of this distribution, which is based on a central-limit argument. Both expressions are then compared to results of numerical simulations in different dynamical regimes of the LIF model.

A. Integral (linear response) approximation

By inserting approximation Eq. (15) into Eq. (5) we obtain an integral expression of the activity distribution, which should be valid for weak input correlation ($c \ll 1$):

$$\hat{p}_A(A) = N\binom{N}{AN}\int_0^1 [R^A(1-R)^{(1-A)}]^N \hat{p}_R(R)dR. \quad (16)$$

Because in the asymptotic limit ($N \to \infty$), $\hat{p}_A$ becomes equal to $\hat{p}_R$ [cf. Eq. (6)], the linear response approximation implies that $\hat{p}_A$ approaches a normal distribution for large N. Hence, for large N the discrepancy between $\hat{p}_A$ and the true distribution is the same as the discrepancy between $\hat{p}_R$ and p_R.

Our result, Eq. (16), still requires the numerical evaluation of an integral. Next we derive a Gaussian approximation for the activity distribution.

B. Gaussian approximation

The population activity Eq. (2) is a sum of stochastic processes,

$$A = \frac{1}{N}\sum_{k=1}^{N} b_k, \quad (17)$$

where $b_k(t) := \int_{t-\Delta}^{t} x_k(t')dt'$ can be considered as a "box train," which equals one, if the kth neuron spiked within $[t-\Delta, t]$ and is zero otherwise. For fixed t, $A(t)$ is a sum of random variables, having similar distributions, which are only weakly correlated due to the common stimulus. Having the central limit theorem in mind, it is plausible to approximate A by a Gaussian process for large N. The mean value of A (average over all noise sources ξ_k, $k \in \{0,1,\ldots N\}$) is given by

$$\langle A\rangle = \frac{1}{N}\sum_{k=1}^{N}\langle R[s]\rangle_s = R_0, \quad (18)$$

where we used that $R[s] = \langle b_k\rangle_{\xi_k}$ by definition Eq. (8) and stationarity. The second moment of A reads

$$\langle A^2\rangle = \frac{1}{N^2}\left[N\langle b_k^2\rangle + N(N-1)\langle b_k b_{k'}\rangle\right],\ k \neq k'.$$

The two factors in the last term can be separately averaged over the independent noise sources ξ_k and $\xi_{k'}$, which yields for each of them the stimulus-conditioned firing rate. Using furthermore that $b_k^2 = b_k$, because $b_k \in \{0,1\}$ we obtain

$$\langle A^2\rangle = \frac{1}{N}(\langle R[s]\rangle_s + (N-1)\langle R[s]^2\rangle_s). \quad (19)$$

This relation for the second moment holds true for arbitrary correlation strength. Using again the linear response ansatz, Eq. (11), $R[s] = R_0 + \hat{s}$, we can further approximate Eq. (19) by

$$\langle A^2\rangle = R_0^2 + c\langle\hat{s}^2\rangle_s\left(1 - \frac{1}{N}\right) + \frac{R_0(1-R_0)}{N}. \quad (20)$$

Hence, if we assume in the case of large N, a normal distribution $\mathcal{N}(\langle A\rangle, \mathrm{var}(A))$ for the population activity, its density can be approximated for weak common stimulus by

$$\hat{p}_{A,G} = \mathcal{N}\left[R_0, c\langle\hat{s}^2\rangle_s\left(1 - \frac{1}{N}\right) + \frac{R_0(1-R_0)}{N}\right]. \quad (21)$$

As N increases to infinity, both approximations, $\hat{p}_A$ and $\hat{p}_{A,G}$, approach a normal distribution centered at the mean windowed firing probability R_0 with a standard deviation of $\sqrt{c\langle\hat{s}^2\rangle_s}$.

C. Comparison to simulation results

In Fig. 7 both approximations, $\hat{p}_A$ and $\hat{p}_{A,G}$, of the activity distribution are compared to simulation results of populations of LIF neurons in the supra- and subthreshold regime and various combinations of population size and correlation strength. In addition, we show the difference of

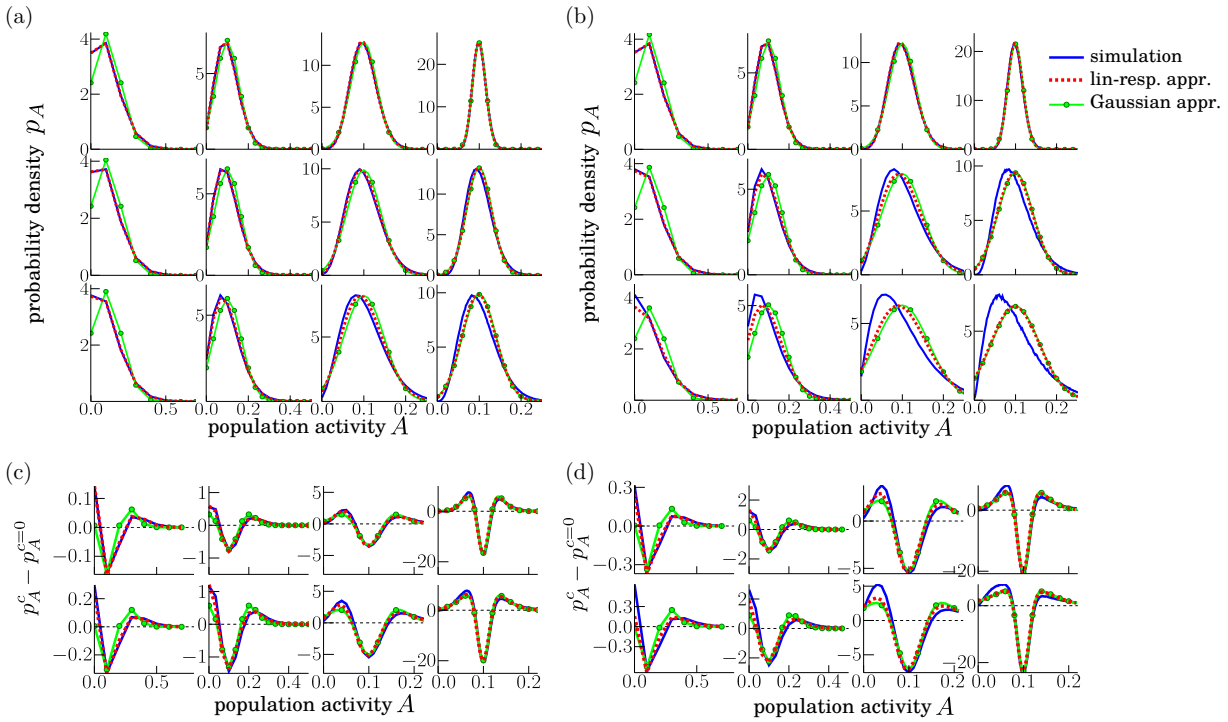

FIG. 7. (Color online) Activity distribution and difference to the uncorrelated case. Comparison of simulation results of the activity distribution (blue/dark gray lines) with the linear response approximation Eq. (16) (red dashed lines) and the Gaussian approximation Eq. (21) (green solid lines with circles) for the suprathreshold (a) and the subthreshold regime (b) of the LIF model for different values of the system size N (from left column to right: $N = 10, 30, 100, 500$) and input correlation c (from top row to bottom: $c = 0.01, 0.1, 0.2$). Respective differences between distributions with and without common noise in (c) and (d) for $c = 0.1$ (top row) and $c = 0.2$ (bottom row). Remaining parameters: $D = 0.01$, $r_0\Delta = 0.1$, $\mu = 1.2$ in (a, c), and $\mu = 0.9$ in (b, d).

the distributions for the activity in the presence and absence of the common stimulus, which directly illustrates the effect of the common drive.

For weak input correlation, $c \ll 1$ (in Figs. 7(a) and 7(b), top row $c = 0.01$) the simulation results are well approximated by the linear response approach, Eq. (16), for all values of the system size. The Gaussian approximation, Eq. (21), works well at larger system size; for instance, the Gaussian is a reasonable description of the histogram for $N \geqslant 30$. As anticipated, both approximations converge for large N.

For larger input correlations, $c = 0.1$ and $c = 0.2$ (Figs. 7(a) and 7(b), middle and bottom rows) there are small deviations between the linear response theory and the simulation results. These deviations are larger for the subthreshold than for the suprathreshold regime and—as can be expected—are larger for $c = 0.2$ than for $c = 0.1$. The main character of the distribution is nevertheless still captured by the linear response theory, which, in particular, nicely predicts the difference between the activity distribution and the distribution of the uncorrelated case [Figs. 7(c) and 7(d)].

It is worth discussing the discrepancies between simulations and theory both for large and small population size. First of all, we recall that for large N, p_A approaches the distribution of the firing probability, p_R. This implies that the deviations of $\hat{p}_A$ and p_A (e.g., for $N = 500$ as in Fig. 7, right column) are the same as those between $\hat{p}_R$ and p_R, which we already observed in Fig. 5. Second, and in marked contrast, at small population size (e.g., $N = 10$ as in Fig. 7, left column) the deviations between the linear response theory, $\hat{p}_A$, and the simulations are extremely small.

Why does the linear response approximation work so well for small populations? For small values of N, the first two moments of the distribution of R matter the most for the activity distribution. For example, for $N = 2$, only the mean and variance of R appear in Eq. (4):

$$p_A\left(A = \frac{m}{2}\right) = 2\binom{2}{m}\langle (R)^m(1-R)^{2-m}\rangle; m \in \{0,1,2\}. \quad (22)$$

The mean, $\langle R\rangle$, is equal to R_0 by construction [cf. Fig. 6(a)] and the variance is well described by the linear response theory up to $c = 0.2$ [cf. Fig. 6(b)]. Hence, p_A is expected to be well described for $N = 2$. For larger N, also higher central moments and by that also higher cumulants will enter Eq. (4), which are not captured by the Gaussian description of p_R. However, their values are much smaller compared to the first two cumulants [see, e.g., the skewness in Fig. 6(c)]. Only when higher-order cumulants make up many terms in Eq. (4), as for larger N, these will notably contribute.

We can quantify the deviations between theory and simulations more systematically. To this end, we use the normalized Jensen-Shannon (JS) divergence [25,31] between the approximation $\hat{p}_A$ and the measured distribution p_A, which is given by

$$\text{JS-div} = \frac{D_{\text{KL}}(p_A||M) + D_{\text{KL}}(\hat{p}_A||M)}{2\ln(N)}, \quad (23)$$

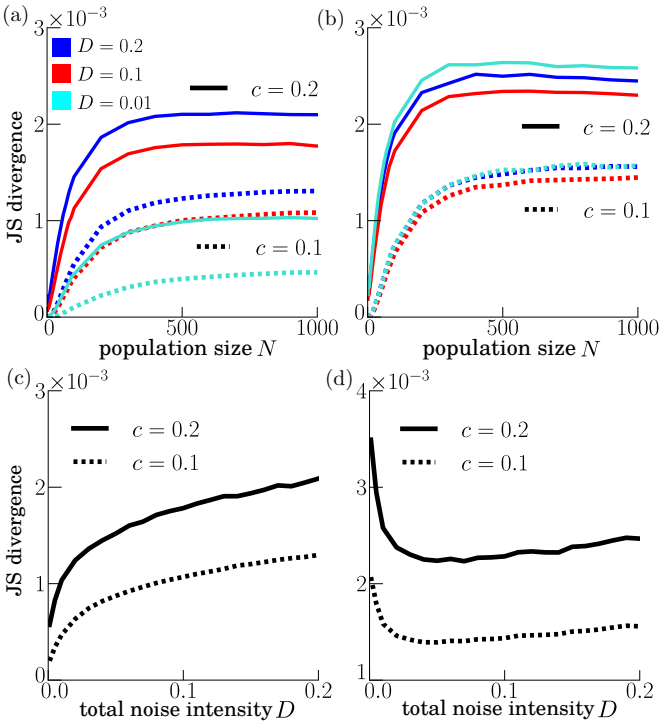

FIG. 8. (Color online) Jensen-Shannon divergence between theory and simulation vs. population size and total noise intensity. JS divergence, Eq. (23), between the simulated population activity distribution p_A and its linear response approximation $\hat{p}_A$ vs. population size for two different input correlations c as indicated (a, b). JS divergence vs. the total noise intensity D for a population of $N = 1000$ neurons (c, d). Remaining parameters: $r_0\Delta = 0.1$, $\mu = 1.2$ in (a, c), and $\mu = 0.9$ in (b, d).

where $M = (p_A + \hat{p}_A)/2$ and

$$D_{\mathrm{KL}}(P||Q) = \frac{1}{N}\sum_{k=0}^{N} P(k)\ln\left[\frac{P(k)}{Q(k)}\right] \qquad (24)$$

is the Kullback-Leibler divergence. The JS divergence quantifies the discrepancy between two probability densities. In Fig. 8 we see that even for moderate input correlations c, the approximation $\hat{p}_A$ is very similar to the real distribution if the population is small enough. As N increases the deviation grows and reaches a plateau (corresponding to the difference between p_R and $\hat{p}_R$) for the considered range of N. For stronger input correlation, the plateau is reached for smaller N.

Finally, we discuss how the range of validity of the approximation depends on the total noise intensity [Figs. 8(c) and 8(d)]. This dependence differs for the suprathreshold and subthreshold firing regimes of the LIF model. Increasing the total noise intensity D has three effects: (i) the mean firing rate grows [32]; (ii) the intrinsic noise is increased, leading to a linearization of the neuron model [30]; (iii) the signal intensity is increased, potentially leading to nonlinear rectification and saturation effects in the modulation of the firing rate. The last effect results in pronounced non-Gaussian features of the firing-rate distribution and leads in the suprathreshold regime to a growth of the JS divergence with increasing noise. Remarkably, we observe a minimum of the divergence in the subthreshold regime at a nonvanishing value of the noise intensity. This implies that our linear response theory works best for an intermediate total noise level.

VI. SUMMARY AND CONCLUSIONS

We have derived analytical results for the activity of a homogeneous population of uncoupled neurons that is driven by a weak time-dependent common stimulus. Our general results, Eq. (16) and Eq. (21) together with Eq. (13) and Eq. (15), require only the knowledge of the average firing rate and the susceptibility of the neuron. Thus, it can be applied to any population model or also to any real cell population, for which these single-cell statistics can be measured or calculated.

In this paper, we tested our results for populations of cells described by the popular leaky integrate-and-fire model with white Gaussian noise. By comparison with numerical simulations, we found an excellent agreement of our theory for weak correlations ($c \ll 1$) and a still reasonable agreement with only minor deviations between theory and simulations for a moderate value of the input correlation coefficient ($c = 0.2$). Because input correlations are typically not strong [20], we believe that the results put forward in our study will be useful to analyze the effect of common noise in biologically relevant situations.

A suitable experimental system where our theory could be tested are *in vitro* neural cultures [33]. In such preparations the connections between neurons can be gradually removed [34], which corresponds for complete removal to our situation of uncoupled neurons. In addition, the activity response to an external common stimulus can be monitored in detail.

Our results will be particularly useful for the problem of how a common stimulus is encoded in the synchronous output of a neural population [22,23]. So far in Ref. [23], the synchronous output was defined by the event that *all* neurons of a population fire in the same time bin. If we relax this assumption by defining the synchronous output by the event that *at least m* out of N neurons fire, the first basic statistics of interest is the mean value of this synchronous output. This mean value can be related to the cumulative distribution of the population activity A, i.e., to an integral over the statistical measure p_A that we have approximated in this paper. Hence, our results will be useful to explore how sensory signals are encoded by neural populations.

ACKNOWLEDGMENT

We would like to acknowledge funding by DFG (Sachbeihilfe LI 1046/2-1) and BMBF 284 (FKZ: 01GQ1001A).

[1] L. Gammaitoni, P. Hänggi, P. Jung, and F. Marchesoni, Rev. Mod. Phys. **70**, 223 (1998).

[2] B. Lindner, J. García-Ojalvo, A. Neiman, and L. Schimansky-Geier, Phys. Rep. **392**, 321 (2004).

[3] M. D. McDonnell and L. M. Ward, Nat. Rev. Neurosci. **12**, 415 (2011).
[4] P. J. Hudson and I. M. Cattadori, Trends Ecol. Evol. **14**, 1 (1999).
[5] L. Chen, R. Wang, T. Zhou, and K. Aihara, Bioinformatics **21**, 2722 (2005).
[6] A. Nandi and B. Lindner, Chem. Phys. **375**, 348 (2010).
[7] B. Doiron, M. J. Chacron, L. Maler, A. Longtin, and J. Bastian, Nature **421**, 539 (2003).
[8] D. S. Goldobin and A. Pikovsky, Phys. Rev. E **71**, 045201 (2005).
[9] W. Braun, A. Pikovsky, M. A. Matias, and P. Colet, Europhys. Lett. **99**, 20006 (2012).
[10] J.-N. Teramae and D. Tanaka, Phys. Rev. Lett. **93**, 204103 (2004).
[11] K. Yoshida, K. Sato, and A. Sugamata, J. Sound. Vib. **290**, 34 (2006).
[12] P. Bressloff and Y. Lai, J. Math. Neurosci. **1**, 2 (2011).
[13] B. Doiron, B. Lindner, A. Longtin, L. Maler, and J. Bastian, Phys. Rev. Lett. **93**, 048101 (2004).
[14] R. F. Galán, N. Fourcaud-Trocme, G. B. Ermentrout, and N. N. Urban, J. Neurosci. **26**, 3646 (2006).
[15] A. Uchida, R. McAllister, and R. Roy, Phys. Rev. Lett. **93**, 244102 (2004).
[16] Z. F. Mainen and T. J. Sejnowski, Science **268**, 1503 (1995).
[17] P. H. E. Tiesinga, Phys. Rev. E **65**, 041913 (2002).
[18] R. Brette and E. Guigon, Neural Comput. **15**, 279 (2003).
[19] M. Shadlen and W. T. Newsome, J. Neurosci. **18**, 3870 (1998).
[20] A. Renart, J. D. L. Rocha, P. Bartho, and L. Hollender, Science **327**, 587 (2010).
[21] E. R. Kandel, J. H. Schwartz, and T. M. Jessel, *Principles of Neural Science* (McGraw-Hill Companies, New York, 2000).
[22] J. W. Middleton, A. Longtin, J. Benda, and L. Maler, J. Neurophysiol. **101**, 1160 (2009).
[23] N. Sharafi, J. Benda, and B. Lindner, J. Comp. Neurosci. **34**, 285 (2013).
[24] S. Amari, H. Nakahara, S. Wu, and Y. Sakai, Neural Comp. **15**, 127 (2003).
[25] D. A. Leen and E. Shea-Brown, J. Math. Neurosci. **5**, 17 (2015).
[26] E. Schneidman, M. J. Berry, R. Segev, and W. Bialek, Nature **440**, 1007 (2006).
[27] W. Gerstner and W. M. Kistler, *Spiking Neuron Models* (Cambridge University Press, Cambridge, 2002).
[28] L. M. Ricciardi, *Diffusion Processes and Related Topics on Biology* (Springer-Verlag, Berlin, 1977).
[29] B. Lindner and L. Schimansky-Geier, Phys. Rev. Lett. **86**, 2934 (2001).
[30] N. Brunel, F. S. Chance, N. Fourcaud, and L. F. Abbott, Phys. Rev. Lett. **86**, 2186 (2001).
[31] J. Lin, IEEE Trans. Info. Theory **37**, 145 (1991).
[32] R. D. Vilela and B. Lindner, Phys. Rev. E **80**, 031909 (2009).
[33] J. G. Orlandi, J. Soriano, E. Alvarez-Lacalle, S. Teller, and J. Casademunt, Nat. Phys. **9**, 582 (2013).
[34] I. Breskin, J. Soriano, E. Moses, and T. Tlusty, Phys. Rev. Lett. **97**, 188102 (2006).